Article

Not peer-reviewed version

Revealing the Critical Role of Global Electron Density Transfer in the Reaction Rate of Polar Organic Reactions within Molecular Electron Density Theory

Luis R. Domingo * and Mar Ríos-Gutiérrez *

Posted Date: 28 March 2024

doi: 10.20944/preprints202403.1766.v1

Keywords: Global electron density transfer; Molecular Electron Density Theory; Polar reactions; Interacting Quantum Atoms; Interacting Quantum Fragments.

 doi:10.20944/preprints202403.1766.v1

Article

Revealing the Critical Role of Global Electron Density Transfer in the Reaction Rate of Polar Organic Reactions within Molecular Electron Density Theory

Luis R. Domingo * and Mar Ríos-Gutiérrez *

Department of Organic Chemistry, University of Valencia, Dr. Moliner 50, 46100 Burjassot, Valencia, Spain.
* Correspondence: luisrdomingo@gmail.com, m.mar.rios@uv.es

Abstract: The critical role of global electron density transfer (GEDT) in increasing the reaction rate of polar organic reactions has been studied within the framework of Molecular Electron Density Theory (MEDT). To this end, the series of the polar Diels-Alder (P-DA) reactions of cyclopentadiene with cyanoethylene derivatives, for which experimental kinetic data are available, have been chosen. A complete linear correlation between the computed activation Gibbs free energies and the GEDT taking place at the polar transition state structures (TSs) is found; the higher the GEDT at the TS, the lower the activation Gibbs free energy. An interacting quantum atoms (IQA) energy partitioning analysis allows establishing a complete linear correlation between the electronic stabilization of the electrophilic ethylene frameworks and the GEDT taking place at the polar TSs. This finding supports Parr's proposal for the definition of the electrophilicity ω index (*J. Am. Chem. Soc.*, **1999,** *121*, 1922). The present MEDT study allows establishing the critical role of the GEDT in the acceleration of polar reactions, since the electronic stabilization of the electrophilic framework with the electron density gain is greater than the destabilization of the nucleophilic one, making a net favorable electronic contribution to the decrease of the activation energy.

Keywords: global electron density transfer; molecular electron density theory; polar reactions; interacting quantum atoms; interacting quantum fragments

1. Introduction

One of the most useful classifications of organic reactions is in non-polar and polar reactions. While non-polar reactions are experienced mainly by hydrocarbons, most polar reactions are characteristic of organic molecules presenting carbon-heteroatom functional groups. Unsaturated hydrocarbon compounds also experience polar reactions when they are adequately substituted by electron-withdrawing (EW) or electron-releasing (ER) groups. The polar character determines the rate of an organic reaction; while non-polar reactions have high activation energies, in general the more polar, the faster the reaction.

The idea of polar reactions in Organic Chemistry was introduced at the beginning of the last century. The introduction of the terms 'nucleophile' and 'electrophile' as chemists use them today is officially attributed to C. K. Ingold [1], who replaced the terms 'anionoid' and 'cationoid' proposed earlier by A. J. Lapworth in 1925 [2]. The nucleophilicity and electrophilicity concepts were further extended to reactions, and thus there are now so-known electrophilic and nucleophilic attacks, additions, substitutions, etc [3] .

From a theoretical point of view, the implementation in 1999 of the Parr's electrophilicity ω index [4] within conceptual DFT [5,6] (CDFT) was a breakthrough in the theoretical understanding of polar reactions. Thus, in 2002, in an attempt to classify the Diels-Alder (DA) reactions within the polar organic reactions, the first scale of the Parr's electrophilicity ω index of organic molecules was

 doi:10.20944/preprints202403.1766.v1

established, allowing to explain the substituent effects on the diene and the ethylene in the reaction rate [7]. The polar reactivity model of DA reactions was extended to [2+2], [3+2], [5+2], and so on, cycloaddition reactions. After the study of many organic reactions, the empirical nucleophilicity *N* index was proposed in 2008 [8] which, together with the electrophilicity ω index, have become powerful tools to study the polar reactivity in Organic Chemistry [9].

DA reactions, reported for the first time by Diels and Alder in 1928 [10], (see Scheme 1) have become one of the most studied organic reactions from a synthetic as well as theoretical point of view [11,12].

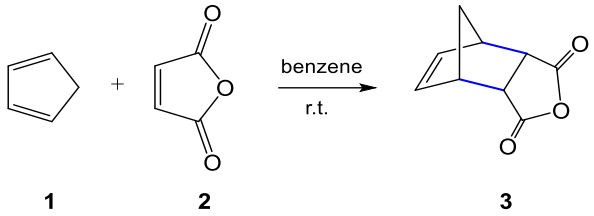

Scheme 1. DA reaction between Cp **1** and maleic anhydride **2**, reported in 1928 by Diels and Alder.

In 1942, Woodward suggested that common experimental DA reactions involve a diene of relatively low ionization potential on the one hand, and a molecule of high electron affinity, e.g. an *α*,*β*-unsaturated carbonyl compound, on the other hand [13]. He proposed a mechanism for experimental DA reactions initiated by an electron transfer from the diene to the dienophile to form an ion-pair intermediate $[A\cdot]^{+}$ $[B\cdot]^{-}$, which further collapses to the final cycloadduct (see Scheme 2). This picture, suggesting a rapid electron transfer process prior to the formation of the new C–C single bonds, was in complete agreement with the large body of observed phenomena associated with the reaction [13]. It is significant to note that species with low ionization potential or with high electron affinity, are related within CDFT to nucleophilic or electrophilic species, respectively [5,6].

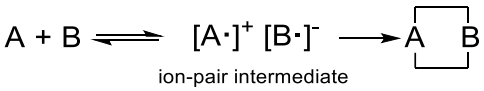

Scheme 2. Woodward's proposed mechanism of experimental DA reactions.

In 1964, Sauer et al. [14] experimentally reported the reactivity of Cp **1** with the cyanoethylene series **4** in DA reactions (see Scheme 3). The reported experimental reaction rate constants have been used in organic chemistry textbooks to show how the EW substitution on the ethylene increases the reaction rates of DA reactions (see Table 1) [12].

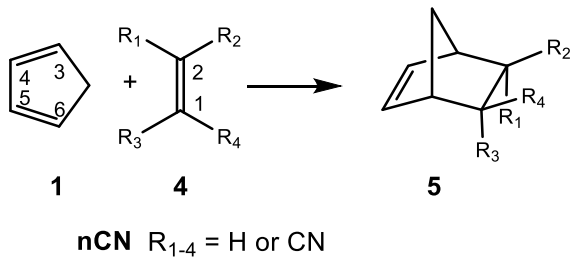

Scheme 3. DA reactions between Cp **1** and the cyanoethylene series **4**, reported in 1964 by Sauer et al.

Table 1. Reaction rate constants for the P-DA reactions of Cp **1** with the cyanoethylene series **4**.[a,b].

	ethylene derivative	10^5k [$M^{-1}s^{-1}$]
4CN	tetracyoanoethylene	4.3 x 10^7
3CN	tricyoanoethylene	4.8 x 10^5

 doi:10.20944/preprints202403.1766.v1

2CN	1,1-dicyoanoethylene	4.5 x 10^4
2cCN	maleonitrile	91
2tCN	fumaronitrile	81
1CN	acrylonitrile	1.04

[a] At 20 °C in dioxane. [b] The rate constant for the Cp **1** + ethylene **6** DA reaction has been estimated in 10^{-5}.

The Sauer's DA reactions of the cyanoethylene series have been theoretically studied [15,16]. A very good linear correlation between the global electron density transfer [17] (GEDT) taking place at the transition state structures (TSs) [15] and the logarithm of the experimental reaction rate constants [14] was established for the first time in 2009 [18], indicating that the GEDT could be one of the key factors in the activation energy (see Figure 1).

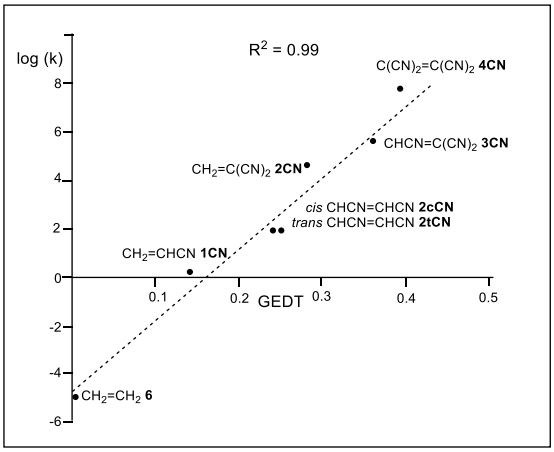

Figure 1. Plot of the logarithm of the experimental reaction rate constant k, in dioxane, vs. GEDT, in average number of electrons, e, for the DA reactions of Cp **1** with ethylene **6** and the cyanoethylene series **4**.

After many theoretical studies of experimental DA reactions, a very good correlation between the activation energies of DA reactions and the GEDT taking place at the TSs was recognized in 2009, thus establishing the general mechanism of polar Diels-Alder (P-DA) reactions [18], which are controlled by the nucleophilic and electrophilic interactions taking place at the TSs. In polar reactions, the increase in GEDT at the TSs causes a decrease in the activation energies, increasing the reaction rates [15,18]. This behavior has been found in many polar organic reactions such as [2+2] [19] and [3+2] [20] cycloaddition reactions, Lewis acid catalyzed DA reactions [21], higher–order cycloaddition reactions [22], Michael reactions [23], Wittig reactions [24], and electrophilic aromatic substitution reactions [25].

In 2016, Domingo proposed the Molecular Electron Density Theory [26] (MEDT) for the study of chemical organic reactivity. MEDT establishes that changes in electron density along a reaction, and not molecular orbital interactions, are responsible for chemical reactivity. Accordingly, MEDT rejects any model based on molecular orbital (MO) analyses such as the Frontier Molecular Orbital (FMO) theory [27] and Morokuma-based energy decomposition schemes [28,29], all of them developed in the last century. To analyze the changes in electron density along an organic reaction, MEDT makes use of a wide range of quantum chemical tools based on the analysis of density functions, such as CDFT [5,6], the electron localization function [30] (ELF), the quantum theory of atoms in molecules [31,32] (QTAIM), and the bonding evolution theory [33] (BET). It is worth noting that although all these tools were proposed during the second half of the last century, they were not practically used in the study of chemical reactivity until the beginning of the current century.

In 2017, a comparative ELF and QTAIM topological analysis of the TSs of the non-polar and polar DA reactions of Cp **1** with ethylene **Et** and with tetracyanoethylene **4CN** was performed to

 doi:10.20944/preprints202403.1766.v1

understand how the GEDT decreases activation energies in P-DA reactions [34]. This earlier MEDT study showed that in the polar reaction involving **4CN**, the GEDT favors the bonding changes on the reagents demanded for the formation of the new C–C single bonds [17], allowing the TS to occur earlier [34]. However, the effects of the GEDT in the reduction of the activation energies could not be established.

In 2005, Blanco et al. developed a parameter-free and reference-free energy decomposition scheme based on QTAIM, called Interacting Quantum Atoms [35] (IQA). IQA divides the total energy of a system into intra- and interatomic contributions of different nature, which are related to chemical concepts of bonding. IQA analysis has very recently been used in MEDT studies of [3+2] cycloaddition reactions [36,37].

Very recently, the catalytic role of the hydrogen-bond (HB) formation in the P-DA reactions of acrolein **7** with Cp **1** has been analyzed within the MEDT (see Scheme 4) [38]. An IQA energy partitioning analysis of the TSs involved in these polar reactions showed that the intra-atomic stabilization of the electrophilic acrolein framework, coupled with the increase of the GEDT at the TSs, plays a critical role in decreasing the activation energies of these HB-catalysed DA reactions, a proposal that was suggested in many earlier theoretical studies [15,18–25].

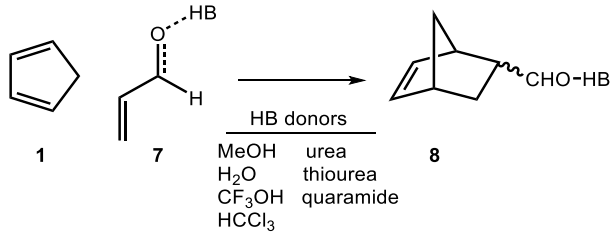

Scheme 4. P-DA reactions of Cp **1** with the HB complexes of acrolein **7**.

Due to the relevance of the GEDT taking place at the TSs of polar reactions in organic chemistry [15,18–25], an MEDT/IQA study of the P-DA reactions of Cp **1** with the Sauer's cyanoethylene series **4**, as models of polar organic reactions, is herein performed in order to definitively establish the critical role of the GEDT in the acceleration in polar processes both qualitatively and quantitatively. To this end, an IQA energy partitioning analysis at the TSs and reagents is carried out. The conclusions of this study can be extrapolated to any organic polar reaction.

2. Results and Discussion

This section has been divided in the following subsections: i) first, the DFT-based reactivity indices of the reagents are analyzed; 2) next, kinetic, thermodynamic and geometrical parameters associated with the P-DA reactions of Cp **1** with the cyanoethylene series **4** are discussed, along with some correlations involving electrophilicities and GEDT values; and finally 3) a density-based energy partitioning analysis is performed in order to establish both quantitatively and qualitatively the role of GEDT in increasing the reaction rates with the cyano substitution on the ethylene. Except for kinetic and thermodynamic data, which are analyzed in dioxane for comparison with experiment, all other analyses are discussed in gas phase for coherence with the IQA analysis, which does not support yet the implicit effect of solvent in atomic integrations (see the Computational Details in Supplementary Material).

2.1. Analysis of the Reactivity Indices at the Ground State (GS) of the Reagents

The reactivity indices [5,6] for Cp **1** and the cyanoethylene series **4** computed at the GS are gathered in Table 2. Computational details are given in Supplementary Material. The B3LYP/6-31G(d) computational method was used because the original reactivity scales were established at that level [5,6]. Analysis of the electronic chemical potentials [39] μ of the regents allows establishing the polar character of an organic reaction, as well as the direction of the flux of the electron density unambiguously, which enable the classification of polar reactions [40]. The electronic chemical

 doi:10.20944/preprints202403.1766.v1

potential μ of Cp **1**, –3.01 eV, is above those of the cyanoethylene series **4**, between –4.70 (**1CN**) and –7.04 (**4CN**) eV, indicating that in these polar reactions the electron density will flux from Cp **1** towards these cyanoethylenes, being classified as P-DA reactions of forward electron density flux (FEDF) [40,41].

Table 2. Gas-phase B3LYP/6-31G(d) global electronic chemical potential μ, chemical hardness η, electrophilicity ω, and nucleophilicity *N*, in eV, of Cp **1** and the cyanoethylene series **4**.

	μ	η	ω	*N*
4CN	-7.04	4.16	5.95	0.00
3CN	-6.43	4.71	4.39	0.33
2tCN	-5.71	5.29	3.08	0.76
2cCN	-5.66	5.32	3.01	0.80
2CN	-5.64	5.65	2.82	0.65
1CN	-4.70	6.34	1.74	1.25
Cp **1**	-3.01	5.49	0.83	3.37
Ethylene **6**	-3.37	7.77	0.73	1.87

Cp **1** presents an electrophilicity ω index [4] of 0.83 eV and a nucleophilicity *N* index [8] of 3.37 eV, being classified as a moderate electrophile and a strong nucleophile. Consequently, Cp **1** will participate in P-DA reactions only as a good nucleophile. On the other hand, ethylene **6** presents an electrophilicity ω index of 0.73 eV and a nucleophilicity *N* index of 1.87 eV, being classified as a marginal electrophile and a marginal nucleophile. Consequently, ethylene **6** will never participate in a P-DA reaction. The non-polar Diels-Alder (N-DA) reaction of Cp **1** with ethylene **6** is classified within MEDT as a null electron density flux (NEDF) reaction [41].

The electrophilicity ω index of cyanoethylene series **4** ranges from 1.74 eV (**1CN**) to 5.95 eV (**4CN**), while the nucleophilicity *N* index ranges from 1.25 eV (**1CN**) to 0.00 eV (**4CN**). Note that the nucleophilicity *N* index for **4CN** is exactly 0.00 eV because this molecule was chosen as the reference for the empirical nucleophilicity *N* scale [6,9]. Thus, while **1CN** is located on the borderline between moderate electrophiles, the other cyanoethylenes are clearly classified as strong electrophiles; note that the tri- and tetracyanoethylenes **3CN** and **4CN**, with ω > 4.0 eV, are classified as superelectrophiles, a behavior that accounts for their high reactivity in polar processes [9] (see Table 1). On the other hand, all cyanoethylenes are classified as marginal nucleophiles. Consequently, this cyanoethylene series will participate towards Cp **1** in P-DA reactions of forward FEDF [41]. Both electrophilic and nucleophilic properties of this series vary with the number of cyano groups on the ethylene.

Along a polar cycloaddition reaction involving non-symmetric species such as **1CN**, **2CN** or **3CN**, the most favorable reaction path involves the two-center interaction with the most electrophilic center of these cyanoethylenes [15]. In this sense, the analysis of the electrophilic P_k^+ Parr functions [42] of the cyanoethylene series is a valuable tool to characterize the most electrophilic center of these molecules (see Figure 2 and Table 3).

Table 3. Gas-phase B3LYP/6-31G(d) electrophilic P_k^+ Parr functions and local electrophilicity ω_k indices at the C1 and C2 carbons of the cyanoethylene series **4**.

	P_k^+		ω_k		$\Delta\omega_k$
	C1	**C2**	**C1**	**C2**	
1CN	0.63	0.20	1.10	0.34	0.76
2cCN	0.35	0.35	0.98	0.98	0.00
2tCN	0.33	0.33	1.01	1.01	0.00
2CN	0.74	0.10	2.28	0.30	1.98

 doi:10.20944/preprints202403.1766.v1

3CN	0.46	0.22	2.03	0.94	1.09
4CN	0.32	0.32	1.91	1.91	0.00

Analysis of the electrophilic P_k^+ Parr functions at the C1 and C2 carbons of the cyanoethylene series **4** indicates that the two ethylene carbons gather more than 60 % of the total amount of spin density in these molecules; i.e. the two carbons will accumulate more than 60 % of the electron density transferred to these ethylene derivatives via the GEDT in these P-DA reactions. As expected, the symmetrically substituted ethylenes **2cCN**, **2tCN** and **4CN** present identical electrophilic P_k^+ Parr functions at the two carbons, while the non-symmetrically substituted **1CN**, **2CN** and **3CN** present a non-symmetrical electrophilic activation; in the three cases, the less substituted carbon present the higher electrophilic P_k^+ Parr function (see Table 3).

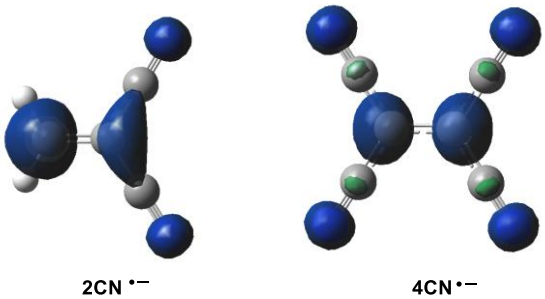

Figure 2. 3D representations of the Mulliken atomic spin densities of the radical anions of **2CN** and **4CN**.

Analysis of the local electrophilicity ω_k indices [43] at the C1 and C2 carbons of these cyanoethylenes allows obtaining some appealing conclusions (see Table 3): i) while the symmetrically substituted ethylenes **2cCN**, **2tCN** and **4CN** present identical electrophilic activation at the two ethylene carbons, predicting synchronous TSs, the non-symmetrically substituted **1CN**, **2CN** and **3CN** present different electrophilic activation, predicting asynchronous TSs [15]; ii) at the non-symmetrically substituted **1CN**, **2CN** and **3CN** cyanoethylenes, the less substituted C1 carbon presents the higher electrophilic activation, indicating that this carbon will be the preferred center to participate in the two-center interaction with the C6 carbon of the nucleophilic Cp **1** [15]; and finally, iii) the local electrophilicity at the C1 carbon of **2CN**, ω_k = 2.28 eV, is higher than that at the C1 carbon of **3CN**, ω_k = 2.03 eV, despite the more electrophilic character of **3CN** than **2CN**. Note that the two C1 and C2 carbons of the symmetrically substituted **2cCN** and **2tCN** are electrophilically activated by ca. ω_k = 1.0 eV each one.

2.2. Study of the P-DA Reactions of Cp 1 with the Cyanoethylene Series 4

For the non-symmetrically substituted cyanoethylenes **1CN**, **2CN** and **3CN**, two stereoisomeric reaction paths are feasible; only the *endo* approach mode was studied herein (see Scheme 3). A detailed analysis of the potential energy surfaces is found in reference 15. The M06-2X/6-311G(d,p) relative Gibbs free energies of TSs and CAs in dioxane are given in Table 4, while complete thermodynamic data are given in Table S3 in Supplementary Material.

The activation Gibbs free energies range from 25.9 (**TS-1CN**) to 12.7 (**TS-4CN**) kcal mol^{-1}. Note that the non-polar (N-DA) reaction of Cp **1** with ethylene **6** displays a very high activation Gibbs free energy of 29.8 kcal mol^{-1} (see Table 4). These DA reactions are exergonic in the narrow range between –12.7 (**CA-1CN**) and –14.9 (**CA-4CN**) kcal mol^{-1}.

 doi:10.20944/preprints202403.1766.v1

Table 4. M06-2X/6-311G(d,p) relative Gibbs free energies (ΔG in kcal mol^{-1}), computed at 293.15 K and 1 atm in dioxane, of TSs and CAs involved in the DA reactions of Cp **1** with ethylene **6** and the cyanoethylene series **4**. The computed relative reaction rate constants k_r, with respect the reaction with ethylene **6**, is also included.

Reagent	TS	ΔG	k_r	Product	ΔG
Ethylene **6**	**TS-Et**	29.8	1.00E+00	**CA-Et**	-12.8
1CN	**TS-1CN**	25.9	8.09E+02	**CA-1CN**	-12.7
2cCN	**TS-2cCN**	22.3	3.91E+05	**CA-2cCN**	-13.8
2tCN	**TS-2tCN**	22.0	6.54E+05	**CA-2tCN**	-14.5
2CN	**TS-2CN**	18.2	4.45E+08	**CA-2CN**	-13.0
3CN	**TS-3CN**	15.9	2.31E+10	**CA-3CN**	-14.9
4CN	**TS-4CN**	12.7	5.62E+12	**CA-4CN**	-14.9

A representation of the activation Gibbs free energies *versus* the number of cyano groups on the ethylene shows a very good linear correlation with a coefficient of determination $R^2 = 0.94$ (see Figure S4 in Supplementary Material). This graph shows that the presence of the cyano group on the ethylene is additive, and has a marked effect on the kinetics of the reactions, in clear agreement with the experimental outcomes observed by Sauer et al. (see Table 1).

Using the Eyring-Polanyi equation [44], the relative reaction rate constants k_r of the P-DA reactions between Cp **1** and the cyanoethylene series **4**, with respect to that with ethylene **5**, were computed (see Table 4). The relative reaction rate constants k_r range from $8.09 \cdot 10^2$ (**1CN**) to $5.62 \cdot 10^{12}$ (**4CN**). Thus, the P-DA reaction involving the superelectrophilic tetracyanoethylene **4CN** is 10^{12} faster than the N-DA reaction of Cp **1** with ethylene **6**. A representation of the logarithm of the experimental relative reaction rate constants log(k_{rexp}), with respect to the N-DA reactions of Cp **1** with ethylene **6**, *versus* the logarithm of the computed relative reaction rate constants log(k_{rcomp}) shows a complete linear correlation with an $R^2 = 1.00$ (see Figure S5 in Supplementary Material).

The main geometrical parameters at the gas phase TSs, i.e. the distances between the two pairs of C1–C6 and C2–C3 interacting centres, together with the geometrical asynchronicity, Δl, and the average of the two C–C distances, lm, are given in Table 5. Geometrical data in dioxane are gathered in Table S4 in Supplementary Material; they show no significant changes compared to the gas phase parameters. The geometries of two representative TSs are given in Figure 3, while the geometries of all TSs are given in Figure S6 in Supplementary Material. Some appealing conclusions can be obtained from the geometrical data given in Table 5: i) from a geometrical point of view, the TSs can be classified as synchronous and asynchronous TSs, depending on the evolution of the new C–C single bond formation; ii) while the synchronous TSs, Δl = 0.0 Å, come from the symmetrically substituted ethylenes, asynchronous TSs, Δl > 0.2 Å, come from the non-symmetrically substituted ethylenes; iii) interestingly, the average of the two C1–C6 and C2–C3 distances at all TS, including **TS-Et**, is 2.24 Å (see lm in Table 5). This behavior indicates that all TSs have a comparable advanced/early character. Considering that the C–C single bond formation takes place in the short range of 2.0-1.9 Å [17], these geometrical parameters indicate that formation of the first C–C single bond has not yet started in any of the TSs (see later). This behavior is consistent with Woodward's 1942 proposal that electron transfer occurs before the formation of the new C-C single bonds [13].

Table 5. Distances between the C1–C6 and C2–C3 interacting carbons at the M06-2X/6-311G(d,p) gas-phase optimized TSs, geometrical asynchronicity Δl, and average of the two C–C interacting distances lm, in angstroms, Å, and GEDT values in average number of electrons, e.

	C1–C6	C2–C3	Δl	lm	GEDT
Et	2.223	2.223	0.00	2.22	0.03
1CN	2.118	2.342	0.22	2.23	-0.14
2cCN	2.220	2.220	0.00	2.22	-0.23

 doi:10.20944/preprints202403.1766.v1

2tCN	2.219	2.233	0.01	2.23	-0.23
2CN	2.025	2.535	0.51	2.28	-0.27
3CN	2.092	2.417	0.32	2.25	-0.34
4CN	2.225	2.225	0.00	2.22	-0.42

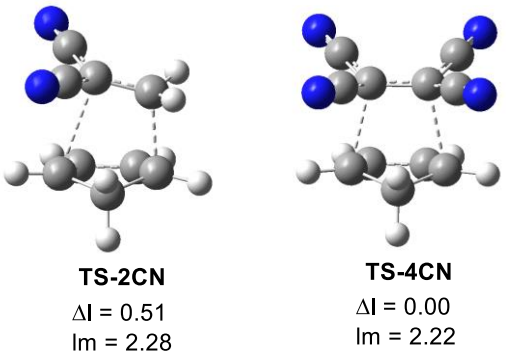

Figure 3. M06-2X/6-311G(d,p) gas-phase optimized geometries of the highly asynchronous **TS-2CN** and the synchronous **TS-4CN**. The geometrical asynchronicity Δl and the average distances, given in angstroms, Å, are also included.

As Figure 4 shows, a complete linear correlation between the geometrical asynchronicity, Δl, of the TSs and the difference of the local electrophilicity ω_k indices of the C1 and C2 carbons of the cyanoethylenes, $\Delta\omega_k$, is established for the first time; R^2 =1.00. Thus, the symmetrically substituted cyanoethylenes **2cCN**, **2tCN** and **4CN** with $\Delta\omega_k$ = 0.00 eV yield synchronous TSs, while non-symmetrically substituted cyanoethylenes **1CN**, **2CN** and **3CN** with $\Delta\omega_k > 0.76$ eV yield asynchronous TSs. This excellent relationship indicates that the different electrophilic activation of the two C1 and C2 carbons of the electrophilic ethylenes caused by the EW substitution controls the asynchronicity of the C–C single bond formation in these P-DA reactions.

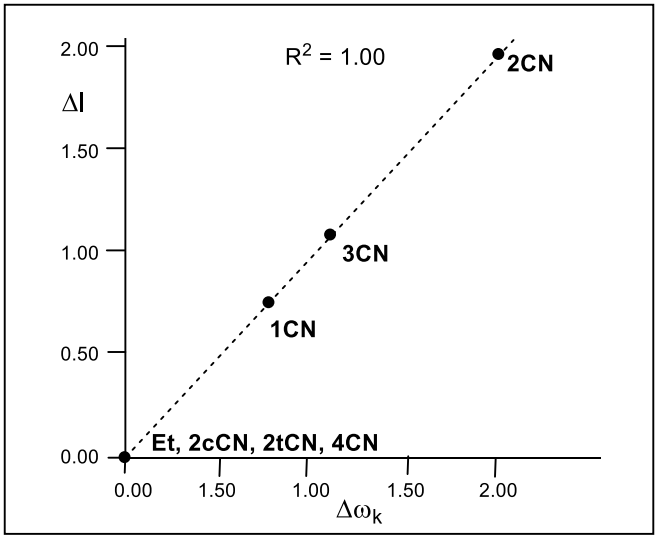

Figure 4. Plot of the gas-phase geometrical asynchronicity of the TSs, Δl in angstroms Å, with respect to the difference of the local electrophilicity ω_k indices of the C1 and C2 carbons of the cyanoethylene series **4**, $\Delta\omega_k$ in eV.

Analysis of GEDT at the TSs permits to quantify the polar character of these DA reactions [17]. The GEDT values computed at the seven TSs in gas phase are given in Table 5. GEDT values in dioxane are displayed in Table S4 in Supplementary Material and show no significant changes compared to the gas-phase values. As expected, the GEDT value at **TS-Et** is negligible, 0.03 e, as a consequence of the marginal electrophilic character of ethylene **5** (see Table 2). Consequently, the

 doi:10.20944/preprints202403.1766.v1

corresponding DA reaction has a non-polar character, being classified as NEDF [41]. The presence of a cyano group in **1CN** notably increases the GEDT at **TS-1CN** to 0.14 e. The addition of cyano groups at the ethylene moiety markedly increases the GEDT at the corresponding TSs, reaching a maximum value at **TS-4CN** with a GEDT = 0.42 e. These P-DA reactions are classified as FEDF [40,41], in agreement with the previous reactivity indices prediction (see Section 2.1). The presence of at least two cyano groups makes the corresponding DA reaction very polar (see Table 5). It is worth mentioning that GEDT values obtained from an NPA analysis do not significantly vary with the charge partitioning method because of its formal definition (see Computational Details). For instance, gas-phase GEDT values computed with Bader charges show no significant variation (see in Table S4 and the linear regression in Figure S7 in Supplementary Material).

A representation of the activation Gibbs free energies of these P-DA reactions *versus* the computed GEDT values at the corresponding TSs also shows a very good linear correlation with an $R^2 = 0.98$ (see Figure 5). This linear correlation, that has been found in numerous organic reactions, shows the significant role of the polar character of the reactions, measured by the computed GEDT values, in reaction rates.

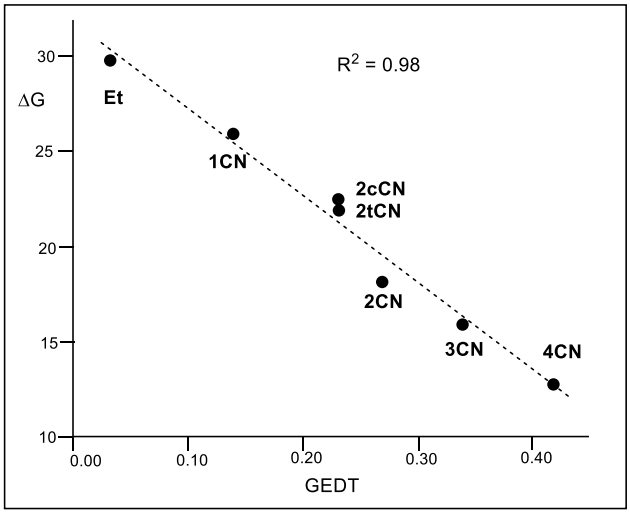

Figure 5. Plot of the M06-2X/6-311G(d,p) activation Gibbs free energies (ΔG in kcal mol^{-1}) vs. the GEDT (in average number of electrons, e), $R^2 = 0.89$, for the DA reactions of Cp **1** with ethylene **6**, and with the cyanoethylene series **4**.

It is worth noting that although geminal **2CN** is less electrophilic than vicinal **2cCN** and **2tCN**, the reaction of **2CN** is more polar and has a higher reaction rate (see Figure 5). This finding points out, once again, the relevant role of GEDT in reaction rates, and indicates that asynchronous processes are generally preferred over synchronous ones due to a more favorable two-center interaction (see later).

Finally, ELF and QTAIM topological analyses of the electronic structures of the reagents and TSs were performed. The corresponding analyses are given in Supplementary Material. ELF analysis of the reagents indicates that the cyano substitution on the ethylene does not cause any remarkable changes in the C–C double bond region at the GS of these substituted ethylenes. On the other hand, ELF analysis of the TSs indicates that while the low polar **TS-1CN** and **TS-2cCN** and **TS-2tCN** shows a great similitude to the non-polar **TS-Et**, the highly polar **TS-2CN**, **TS-3CN** and **TS-4CN** show the presence of the *pseudoradical* centers demanded for the subsequent C–C single bond formation [17]. Both ELF and QTAIM analyses of the electron density at the TSs indicate that formation of the C–C single bonds has not started yet in any of them, thus rejecting the concept of concerted TSs.

2.3. IQA Analysis of the TSs of the P-DA Reactions of the Cyanoethylene Series 4

In order to determine the role of the GEDT caused by the cyano substitution on the ethylene in the experimental acceleration observed by Sauer et al. (see Table 1), a topological IQA [35] energy

 doi:10.20944/preprints202403.1766.v1

partitioning was carried out at the seven TSs in gas-phase. For this purpose, an Interacting Quantum Fragments (IQF) approach [45] was adopted, considering relative IQA energies at both interacting frameworks as defined Supplementary Material. The relative total, intra- and interatomic IQA energies of each TS fragment are given in Table 6, while total values are given in Table S5 in Supplementary Material.

Table 6 shows that the stabilization of the ethylene framework with the number of cyano groups, $\Delta E_{tot}(nCN) < 0$, is stronger than the Cp destabilization, $\Delta E_{tot}(Cp) > 0$, justifying the decrease of the activation energies along this cyanoethylene series. In addition, while the increase of the cyano substitution in the ethylene generally increases $E_{intra}(X)$ in the two interacting frameworks and $V_{inter}(Cp)$, a huge decrease of the interatomic $V_{inter}(nCN)$ energies, by between –16.0 (**1CN**) and –102.0 (**4CN**) kcal mol^{-1}, is observed (see the differences between $V_{inter}(nCN)$ and $V_{inter}(Et)$).

Table 6. M06-2X/6-311G(d,p) gas-phase relative total $E_{tot}(X)$, intra-atomic $E_{intra}(X)$ and interatomic $V_{inter}(X)$ IQA energies, in kcal mol^{-1}, of the cyclopentadiene and ethylene frameworks at the TSs with respect to the separated reagents. The sum of the relative total IQA energies of the two interacting moieties, $E_{tot}(Cp+Et)$, yields the activation energy. Standard deviations are given with respect to the N-DA reaction of Cp **1** with ethylene **6**, in kcal mol^{-1}.

		$E_{intra}(X)$	$V_{inter}(X)$	$E_{tot}(X)$	$E_{tot}(Cp+Et)$
TS-Et	Cp	34.6	-26.8	7.8	15.6
	Et	33.1	-25.3	7.8	
TS-1CN	Cp	37.8	-19.9	17.9	11.0
	1CN	34.4	-41.3	-6.9	
TS-2cCN	Cp	42.3	-13.6	28.7	8.1
	2cCN	49.4	-70.0	-20.6	
TS-2tCN	Cp	41.8	-13.2	28.6	6.9
	2tCN	46.5	-68.2	-21.7	
TS-2CN	Cp	41.2	-10.0	31.2	4.0
	2CN	29.3	-56.5	-27.2	
TS-3CN	Cp	46.1	-4.4	41.7	1.9
	3CN	54.8	-94.6	-39.8	
TS-4CN	Cp	51.9	1.3	53.2	-1.5
	4CN	72.6	-127.3	-54.7	
Standard deviation	Cp	10.0	18.2	28.1	
	nCN	20.4	58.1	39.3	

Figure 6 shows a graphical representation of the IQF $E_{tot}(X)$ energy of the Cp and Et frameworks at the seven TSs and the $E_{tot}(Cp+Et)$, which corresponds to the activation energies of these DA reactions. As can be observed, both $E_{tot}(X)$ are positive and unfavorable in the N-DA reaction with ethylene **6**. However, along the cyanoethylene series **4**, the IQF energies associated with the Cp framework increase while those of the ethylene derivatives become more negative, i.e. more stabilizing. This stabilization reaches such an extent that, in **TS-4CN**, the stabilization of the ethylene framework overcomes the destabilization of the Cp one, and the corresponding relative energy of **TS-4CN** becomes negative. These behaviors are a consequence of the GEDT that takes place at the TSs (see Figure 6), that while it destabilizes the nucleophile Cp for making it lose electron density, it stabilizes the electrophile nCN as it gains electron density.

 doi:10.20944/preprints202403.1766.v1

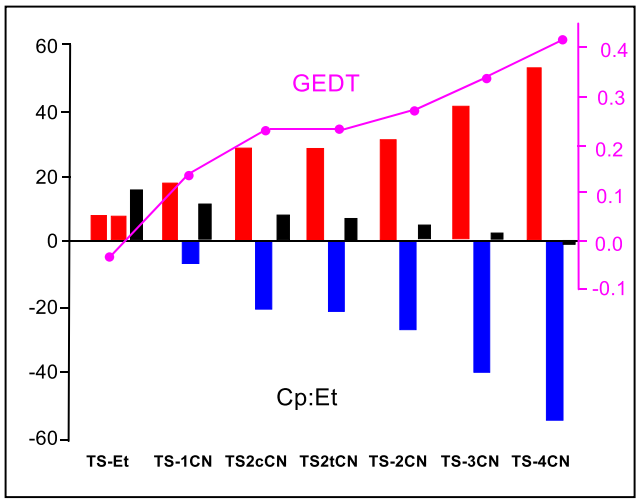

Figure 6. Graphical representation of the sets of E_{tot}(Cp), E_{tot}(Et), and E_{tot}(Cp+Et) energies in that order for the TSs associated with the DA reactions of Cp **1** with ethylene **6** and the cyanoethylenes series **4**. E_{tot}(Cp+Et) corresponds to the activation energies of the reactions. The GEDT values at the TSs are given in pink. E_{tot}(X) energies are given in kcal mol^{-1}, and the GEDT in average number of electrons, e.

Consequently, the strong stabilization of the cyanoethylene framework at the TSs with the cyano substitution, by between 14.7 (**1CN**) and 62.5 (**4CN**) kcal mol^{-1} with respect to the N-DA reaction of Cp **1** with ethylene **6**, accounts for the decrease of the activation energies associated with the P-DA reactions between Cp **1** and the cyanoethylene series **4**.

A representation of the logarithm of the experimental reaction rate constant k versus the stabilization of the ethylene frameworks at the TSs shows an excellent linear correlation with an R^2 = 0.95 (see Figure S8 in Supplementary Material). This figure shows the close relationship between the experimentally observed acceleration in this series of P-DA reactions and the decrease in activation energy resulting from the electronic stabilization of the ethylene framework. Furthermore, a representation of E_{tot}(Et) versus the GEDT computed at the TSs shows an excellent linear correlation with an R^2 = 0.99 (see Figure 7).

These linear correlations allow establishing, for the first time, that the electronic stabilization of the ethylene framework, resulting from the GEDT process taking place in polar reactions, is responsible for the increase of the reaction rate observed in these polar reactions [18]. Note that the N-DA reaction of ethylene **6**, which presents a GEDT = 0.03 e, fits in the top left corner in the linear regression in Figure 7.

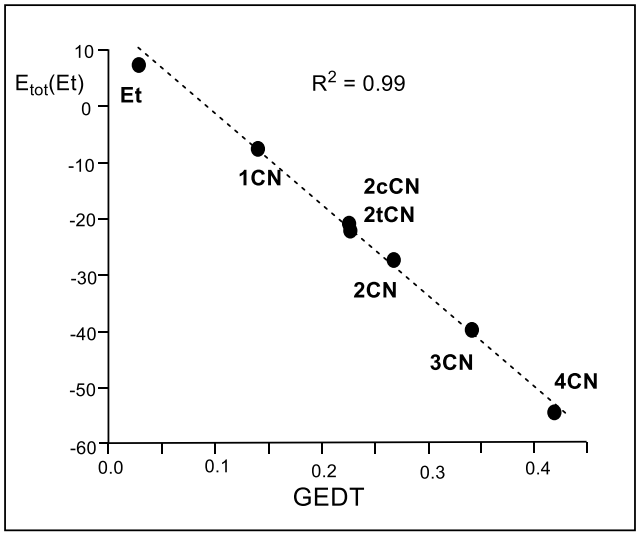

 doi:10.20944/preprints202403.1766.v1

Figure 7. Plot of the gas-phase M06-2X/6-311G(d,p) relative total IQA atomic energies of the ethylene framework (E_{tot}(Et) in kcal mol^{-1}) vs. the GEDT (in average number of electrons, e) for the DA reactions of Cp **1** with ethylene **6** and the cyanoethylene series **4**.

As the energy factor that changes the most with the cyano substitution is V_{inter}(Et), in order to gain a more detailed insight into the stabilization of the ethylene derivatives, the interatomic interactions between the Cp and ethylene frameworks, V_{inter}(Cp,Et), were considered separately from the interactions that take place within each of them, V'_{inter}(X). The corresponding energies, together with the standard deviations with respect to the N-DA reaction of ethylene **6** as the reference, are given in Table 7.

The standard deviation values indicate that the most drastic changes with the cyano substitution take place in decreasing the interatomic interactions occurring inside the ethylene fragment (see the standard deviation of V'_{inter}(Et) in Table 7). This effect overcomes the changes in the interatomic interactions between the fragments, V_{inter}(Cp,Et), which also become more stabilizing as the polar character of the reaction increases.

These findings confirm that the stabilization of the electrophilic reagent in P-DA reactions is the most relevant consequence of the GEDT, thus being responsible for the increase of reaction rates with the increase of the polar character [17].

Table 7. M06-2X/6-311G(d,p) gas-phase total interatomic interactions between the two Cp and Et fragments, V_{inter}(Cp,Et), and relative total interatomic energies within the two Cp and Et frameworks, V'_{inter}(X), in kcal mol^{-1}. Relative energies are given with respect to the separated reagents. Standard deviations are given with respect to the N-DA of Cp **1** with ethylene **6**, in kcal mol^{-1}.

	V_{inter}(Cp,Et)	V'_{inter}(Cp)	V'_{inter}(Et)
TS-Et	-153.7	50.0	51.5
TS-1CN	-160.4	60.4	38.9
TS-2cCN	-167.7	70.3	13.7
TS-2tCN	-168.7	71.1	16.2
TS-2CN	-165.5	72.8	26.3
TS-3CN	-174.1	82.6	-7.6
TS-4CN	-187.3	94.8	-33.6
Deviation	18.9	27.5	48.7

Finally, in 1999, Parr proposed the electrophilicity index ω as a measure of the electronic stabilization of a species when it acquires a certain amount of electron density from the environment [4]. Thus, when the sum of the relative intra-atomic E_{intra}(Et) and interatomic V'_{inter}(Et) IQA energies, i.e. E'_{tot}(Et), are represented versus the corresponding Parr's electrophilicity ω indices (see Table 2), a very good linear correlation is obtained; R^2 = 0.97 (see Figure 8). The E'_{tot}(Et) in the N-DA reaction between Cp **1** and ethylene **6** is very unfavorable, 84.6 kcal mol^{-1}. The inclusion of the cyano groups stabilize the ethylene framework at the TSs by between 11.3 (**1CN**) and 45.7 (**4CN**) kcal mol^{-1} as a consequence of the GEDT taking place at the polar TSs (see Figure 8). Consequently, this graph supports Parr's proposal [4,46]; the higher the electrophilicity ω index, the higher the ethylene stabilization at the polar TSs. Given that the ethylene stabilization via the GEDT is the main factor responsible for the decrease of activation energies, as shown above, this linear correlation also validates Parr's electrophilicity ω index as a solid predictor of reactivity in polar cycloaddition reactions.

 doi:10.20944/preprints202403.1766.v1

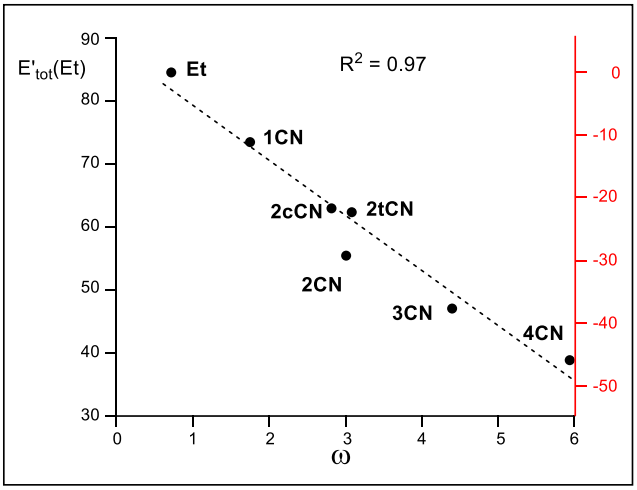

Figure 8. Plot of the M06-2X/6-311G(d,p) gas-phase relative total IQA energy at the ethylene framework, $E'_{tot}(Et)$ in kcal mol^{-1}, vs. Parr's electrophilicity ω indices (in eV) of the ethylenes involved in the DA reactions of Cp **1** with ethylene **6** and the cyanoethylene series **4**. The scale of the energy differences with respect to the N-DA reaction of ethylene **6**, which measure the TS stabilization, is given in red on the right side.

3. Computational Methods

The M06-2X functional [47], together with the standard 6-311G(d,p) basis set [48], which includes d-type polarization for second-row elements and p-type polarization functions for hydrogens, was used throughout this MEDT study. The TSs were characterized by the presence of only one imaginary frequency.

Solvent effects of dioxane were taken into account in the thermodynamic calculations by full optimization of the gas-phase structures at the same computational level using the polarizable continuum model (PCM) [49,50] in the framework of the self-consistent reaction field (SCRF) [51,53] Values of M06-2X/6-311G(d,p) enthalpies, entropies, and Gibbs free energies in dioxane were calculated with standard statistical thermodynamics[2] at 293.15 ºC and 1 atm by PCM frequency calculations at the solvent-optimized structures. Except thermodynamic data, the rest of the results are obtained in gas phase for an overall coherence in interpreting the results obtained from different quantum chemical tools

DFT reactivity indices were calculated using the equations in reference 6. The GEDT [17] values were computed using the equation $GEDT(f) = \Sigma q_f$, where q are the natural charges [54,55] of the atoms belonging to one of the two frameworks (f) at the TS geometries.

The Gaussian 16 suite of programs was used to perform the calculations [56]. Molecular geometries were visualized by using the GaussView program [57]. ELF analyses [30] of the M06-2X/6-311G(d,p) monodeterminantal wavefunctions were done by using the TopMod [58] package with a cubical grid of step size of 0.1 Bohr. Molecular geometries and ELF basin attractors were visualized by using the GaussView program The Bader's QTAIM [30,31] analyses were conducted using Multiwfn 3.7 software packages [59] The IQA [35] analysis was performed with the AIMAll package [60] using the corresponding M06-2X/6-311G(d,p) monodeterminantal wavefunctions.

4. Conclusions

The critical role of the GEDT in increasing the reaction rate of polar reactions has been studied within the MEDT. To this end, the P-DA reactions of Cp **1** with the cyanoethylene series **4**, experimentally studied by Sauer [14], have been chosen as polar reaction models. Concepts developed in the last years in the field of theoretical organic chemistry permits a rationalization of the behaviors of these P-DA reactions.

 doi:10.20944/preprints202403.1766.v1

A complete linear correlation between the activation Gibbs free energies associated with these P-DA reactions and the GEDT values calculated at the TSs is found. This very good correlation, which has also been found for many organic reactions, allows the GEDT to be established as a critical factor in the acceleration experimentally found in polar organic reactions.

The present study shows that the asynchronicity in P-DA reactions depends on the non-symmetric electrophilic activation of the two interacting carbons of the ethylene caused by the EW substitution. A very good linear correlation between the geometric asynchronicity, Δl, of the TSs and the difference in the local electrophilicity ω_k indices of the C1 and C2 carbons of the cyanoethylenes, $\Delta\omega_k$, is found.

An IQA/IQF energy partitioning analysis of the TSs permits to establish the decisive role of the GEDT in the acceleration found in polar reactions. The topological IQA energy partitioning allows establishing the complete linear correlation between the total IQA atomic energies of the electrophilic ethylene framework and the GEDT taking places ta the TSs of these P-DA reactions of FEDF. This finding established that the increase in GEDT at the TSs enhances the reaction rates of P-DA reactions through an electronic stabilization of the electrophilic framework.

Finally, the very good linear correlation found between the sum of the relative intra- and interatomic IQA energies of the atoms belonging to the electrophilic ethylene frameworks and the Parr's electrophilicity ω indices of the cyanoethylene series **4** involved in these P-DA reactions supports Parr's proposal made in 1999 for the definition of this relevant reactivity index [4].

Supplementary Materials: The following supporting information can be downloaded at the website of this paper posted on Preprints.org. ELF and QTAIM topological analysis of the TSs. References. Figure S4 with the plot of the computed M06-2X/6-311G(d,p) activation Gibbs free energies versus the number of cyano groups on the ethylene for the DA reactions of Cp **1** with the cyanoethylene series **4**. Figure S5 with the plot of the logarithm of the experimental relative reaction rate constants versus the logarithm of the computed M06-2X/6-311G(d,p) relative reaction rate constants for the DA reactions of Cp **1** with the cyanoethylene series **4**. Figure S6 with the M06-2X/6-311G(d,p) gas phase optimized geometries of the TSs involved in the DA reactions of Cp **1** with ethylene **6** and the cyanoethylene series **4**. Figure S7 with the plot of the gas-phase GEDT obtained by using Bader charges with respect to gas-phase GEDT obtained by using NPA charges. Figure S8 with the plot of the logarithm of the experimental reaction rate constants versus relative total IQA atomic energies stabilization of the ethylene framework for the DA reactions of Cp **1** with the cyanoethylene series **4**. Table S2 with the M06-2X/6-311G(d,p) gas phase total electronic energies of reagents, TSs and CAs involved in the DA reactions of Cp **1** with ethylene **6** and the cyanoethylene series **4**. Table S3 with the M06-2X/6-311G(d,p) enthalpies, entropies and Gibbs free energies, computed at 293.15 K and 1 atm in dioxane, for the stationary points involved in the DA reactions of Cp **1** with ethylene **6** and the cyanoethylene series **4**. Table S4 with distances between the C1–C6 and C2–C3 interacting carbons at the M06-2X/6-311G(d,p) optimized TSs in dioxane, geometrical asynchronicity, average of the two C–C interacting distances, and GEDT values. Table S5 with the total intra- and interatomic IQA energies at the diene and ethylene frameworks of the TSs and at the reagents involved in the DA reactions of Cp **1** with ethylene **6** and the cyanoethylene series **4**. M06-2X/6-311G(d,p) gas phase computed total energies, single imaginary frequencies of TSs, and Cartesian coordinates of the stationary points involved in the DA reactions of Cp **1** with ethylene **6** and the cyanoethylene series **4**.

Author Contributions: Conceptualization, L.R.D.; methodology, L.R.D. and M.R.G.; software, X.X.; validation, L.R.D. and M.R.G.; formal analysis, L.R.D. and M.R.G.; investigation L.R.D. and M.R.G.; data curation, L.R.D. and M.R.G.; writing—original draft preparation, L.R.D. and M.R.G.; writing—review and editing, L.R.D. and M.R.G.; visualization, L.R.D. and M.R.G. supervision, L.R.D. and M.R.G. All authors have read and agreed to the published version of the manuscript.

Funding: This research received no external funding.

Data Availability Statement: The data that support the findings of this study are available from the corresponding author upon reasonable request.

Conflicts of Interest: The authors declare no conflicts of interest.

References

1. Ingold, C.K. Significance of tautomerism and of the reactions of aromatic compounds in the electronic theory of organic reactions. *J. Chem. Soc.* **1933**, 1120-1127.
2. Lapworth, A. Replaceability of Halogen Atoms by Hydrogen Atoms, *Nature*, **1925**, *115*, 625.
3. Carey, F.A.; Sundberg, R.J. *Advanced Organic Chemistry, Part A: Structure and Mechanisms.* Springer, New York, 2008.
4. Parr, R.G.; Szentpaly, L.v.; Liu, S. Electrophilicity index. *J. Am. Chem. Soc.* **1999**, *121*, 1922-1924.
5. Parr, R.G.; Yang, W. *Density functional theory of atoms and molecules.* Oxford University Press, New York, 1989.
6. Domingo, L.R.; Ríos-Gutiérrez, M.; Pérez, P. Applications of the conceptual density functional indices to organic chemistry reactivity. *Molecules* **2016**, *21*, 748.
7. Domingo, L.R.; Aurell, M.J.; Pérez, P.; Contreras, R.Quantitative characterization of the global electrophilicity power of common diene/dienophile pairs in Diels–Alder reactions. *Tetrahedron* **2002**, *58*, 4417-4423.
8. Domingo, L.R.; Chamorro, E.; Pérez, P. Understanding the reactivity of captodative ethylenes in polar cycloaddition reactions. A theoretical study. *J. Org. Chem.* **2008**, *73*, 4615-4624.
9. Domingo, L.R.; Ríos-Gutiérrez, M. In Application of Reactivity Indices in the Study of Polar Diels–Alder Reactions. *Conceptual Density Functional Theory: Towards a New Chemical Reactivity Theory*, Ed. Shubin Liu. WILEY-VCH GmbH. 2022, Vol. 2, pp. 481-502.
10. Diels, O.; Alder, K. Synthesen in der hydroaromatischen Reihe. *Justus Liebigs Ann. Chem.* **1928**, *460*, 98-122.
11. Carruthers, W. In *Some Modern Methods of Organic Synthesis*. 2nd ed.; Cambridge University Press: Cambridge, UK, 1978.
12. Carruthers, W. In *Cycloaddition Reactions in Organic Synthesis*. Pergamon: Oxford, UK, 1990.
13. Woodward, R.B. The mechanism of the Diels-Alder reaction. *J. Am. Chem. Soc.*, **1942**, *64*, 3058–3059.
14. Sauer, J.; Wiest, H.; Mielert, A. Eine Studie der Diels-Alder-Reaktion, I. Die Reaktivität von Dienophilen gegenüber Cyclopentadien und 9.10-Dimethyl-anthracen. *Chem. Ber.* **1964**, *97*, 3183–3207.
15. Domingo, L.R.; M. J. Aurell, Pérez, P.; Contreras, R. Origin of the synchronicity on the transition structures of polar Diels-Alder reactions. Are these reactions [4+2] processes?. *J. Org. Chem.* **2003**, *68*, 3884–3890.
16. Jones, G.O.; Guner, V.A.; Houk, K.N. Diels-Alder Reactions of Cyclopentadiene and 9,10-Dimethylanthracene with Cyanoalkenes: The Performance of Density Functional Theory and Hartree-Fock Calculations for the Prediction of Substituent Effects. *J. Phys. Chem. A* **2006**, *110*, 1216-1224.
17. Domingo, L.R. A new C-C bond formation model based on the quantum chemical topology of electron density. *RSC Adv.* **2014**, *4*, 32415-32428.
18. Domingo, L.R.; Sáez, J.A. Understanding the mechanism of polar Diels-Alder reactions. *Org. Biomol. Chem.* **2009**, *7*, 3576–3583.
19. Arnó, M.; Zaragozá, R.J.; Domingo, L.R. Lewis acid induced [2+2] Cycloadditions of Silyl Enol Ethers with ⍵⍵⍵-Unsaturated Esters. A DFT Analysis. *Eur. J. Org. Chem.* **2005**, 3973-3979.
20. Domingo, L.R.; Ríos-Gutiérrez, M.; Pérez, P. A Molecular Electron Density Theory Study of the Reactivity and Selectivities in [3+2] Cycloaddition Reactions of C,N-Dialkyl Nitrones with Ethylene Derivatives. *J. Org. Chem.* **2018**, *83*, 2182-2197.
21. Domingo, L.R.; Ríos-Gutiérrez, M.; Pérez, P. Unveiling the Lewis Acid Catalysed Diels–Alder Reactions Through the Molecular Electron Density Theory. *Molecules* **2020**, *25*, 2535.
22. Domingo, L.R.; Pérez, P. Understanding the Higher–Order Cycloaddition Reactions of Heptafulvene, Tropone and its Nitrogen Derivatives with Electrophilic and Nucleophilic Ethylenes inside the Molecular Electron Density Theory. *New J. Chem.* **2022**, *46*, 294-308.
23. Domingo, L.R.; Seif, A.; Mazarei, E.; Zahedi, E.; Ahmadi, T.S. A Molecular Electron Density Theory (MEDT) study of the role of halogens (X2= F2, Cl2, Br2 and I2) on the aza-Michael-addition reactions. *New J. Chem.* **2020**, *44*, 19002-19012.
24. Chamorro, E.; Duque-Norena, M.; Gutiérrez-Sanchez, N.; Rincon, E.; Domingo, L.R. A close look to the oxaphosphetane formation along the Wittig reaction: A [2+2] cycloaddition? *J. Org. Chem.* **2020**, *85*, 6675-6686.
25. Domingo, L.R.; Aurell, M.J. Unveiling the Electrophilic Aromatic Substitution Reactions of Pyridine Derivatives with Nitronium Ion through Molecular Electron Density Theory. *New. J. Chem.* **2023**, *47*, 5193-5202.
26. Domingo, L.R. Molecular Electron Density Theory: A Modern View of Reactivity in Organic Chemistry. *Molecules* 2016, **21**, 1319.
27. Fukui, K. In *Molecular Orbitals in Chemistry, Physics, and Biology*, New York, 1964.

28. Kitaura, K.; Morokuma, K. A new energy decomposition scheme for molecular interactions within the Hartree-Fock approximation. *Int. J. Quantum Chem.* **1976**, *10*, 325-340.
29. Morokuma, K.; Kitaura, K. In *Chemical Applications of Atomic and Molecular Electrostatic Potentials*, New York, Plenum., 1981, pp. 215–242.
30. Becke, A.D.; Edgecombe, K.E. A simple measure of electron localization n atomic and molecular-systems. *J. Chem. Phys.* **1990**, *92*, 5397–5403.
31. Bader, R.F.W.: Tang, Y.H.; Tal, Y.; Biegler-König, F.W. Properties of atoms and bonds in hydrocarbon molecules. *J. Am. Chem. Soc*. **1982**, *104*, 946–952.
32. Bader, R.F.W. Atoms in Molecules: A Quantum Theory. Oxford University Press, Oxford, New York, 1994.
33. Krokidis, K.; Noury, S.; Silvi, B. Characterization of Elementary Chemical Processes by Catastrophe Theory. *J. Phys. Chem. A.* **1997**, *101*, 7277–7282.
34. Domingo, L.R.; Ríos-Gutiérrez, M.; Pérez, P. How does the global electron density transfer diminish activation energies in polar cycloaddition reactions? A Molecular Electron Density Theory study. *Tetrahedron* **2017**, *73*, 1718-1724.
35. Blanco, M.A.; Martín Pendás, A.; Francisco, E. Interacting Quantum Atoms: A Correlated Energy Decomposition Scheme Based on the Quantum Theory of Atoms in Molecules. *J. Chem. Theory Comput.* **2005**, *1*, 1096–1109.
36. Ríos-Gutiérrez, M.; Falcioni, F.; Domingo, L.R.; Popelier, P.L.A. A Combined BET and IQA-REG Study of the Activation Energy of non-polar zw-type [3+2] Cycloaddition Reactions. *Phys. Chem. Chem. Phys.* 2023, **25**, 10853–10865.
37. Domingo, L.R.; Ríos-Gutiérrez, M.; Pérez, P. Why is Phenyl Azide so Unreactive in [3+2] Cycloaddition Reactions? Demystifying Sustmann's Paradigmatic Parabola. Org. Chem. Front. 2023, 10, 5579–5591.
38. Domingo, L.R.; Pérez, P.; Ríos-Gutiérrez, M.; Aurell, M.J. A Molecular Electron Density Theory Study of Hydrogen Bond Catalysed Polar Diels–Alder Reactions of α,β-unsaturated Carbonyl Compounds. *Tetrahedron Chem.* **2024**, *10*, 100064.
39. Parr, R.G.; Pearson, R.G. Absolute hardness: Companion parameter to absolute electronegativity. *J. Am. Chem. Soc.* 1983, **105**, 7512–7516.
40. Domingo, L.R.; Ríos-Gutiérrez, M.; Pérez, P. A Molecular Electron Density Theory Study of the Reactivity of Tetrazines in Aza-Diels-Alder Reactions. *RSC Adv.* **2020**, *10*, 15394–15405.
41. Domingo, L.R.; Ríos-Gutiérrez, M. A Useful Classification of Organic Reactions Bases on the Flux of the Electron Density. *Sci. Rad.* **2023**, *2*, 1.
42. Domingo, L.R.; Pérez, P.; Sáez, J.A. Understanding the local reactivity in polar organic reactions through electrophilic and nucleophilic Parr functions. *RSC Adv.* **2013**, *3*, 1486–1494.
43. Domingo, L.R.; Aurell, M.J.; Pérez, P.; Contreras, R. Quantitative characterization of the global electrophilicity power of common diene/dienophile pairs in Diels–Alder reactions. *Tetrahedron* **2002**, *58*, 4417–4423.
44. Evans, M.G.; Polanyi, M. Some applications of the transition state method to the calculation of reaction velocities, especially in solution. *Trans. Faraday Soc.* **1935**, *31*, 875–894.
45. Triestram, L.; Falcioni, F.; Popelier, P.L.A. Interacting Quantum Atoms and Multipolar Electrostatic Study of XH···π Interactions. *ACS Omega* **2023,** *8*, 34844–34851.
46. Chattaraj, P.K.; Roy, D.R. Update 1 of: Electrophilicity Index. *Chem. Rev.* **2007**, 107, PR46–PR74.
47. Zhao, Y.; Truhlar, D. G.The M06 suite of density functionals for main group thermochemistry, thermochemical kinetics, noncovalent interactions, excited states, and transition elements: two new functionals and systematic testing of four M06-class functionals and 12 other functionals. *Theor. Chem. Acc.* **2008**, *120*, 215-245.
48. Hehre, M.J.; Radom, L.; Schleyer, P.V.R.; Pople, J. *Ab initio Molecular Orbital Theory*. Wiley: New York, NY, USA, 1986.
49. Tomasi, J.; Persico, M. Molecular interactions in solution: And overview of methods based on continuous distributions of the solvent. *Chem. Rev.* **1994**, *94*, 2027–2094.
50. Simkin, B.Y.; Sheikhet, I.I. *Quantum Chemical and Statistical Theory of Solutions–Computational Approach*. Ellis Horwood: London, UK, 1995.
51. Cossi, M.; Barone, V.; Cammi, R.; Tomasi, J. Ab initio study of solvated molecules: A new implementation of the polarizable continuum model. *Chem. Phys. Lett.* **1996**, *255*, 327–335.
52. Cances, E.; Mennucci, B.; Tomasi, J. A new integral equation formalism for the polarizable continuum model: Theoretical background and applications to isotropic and anisotropic dielectrics. *J. Chem. Phys.* **1997**, *107*, 3032–3041.

 doi:10.20944/preprints202403.1766.v1

53. Barone, V.; Cossi, M.; Tomasi, J. Geometry optimization of molecular structures in solution by the polarizable continuum model. *J. Comput. Chem.* **1998**, *19*, 404–417.
54. Reed, A.E.; Weinstock, R.B.; Weinhold, F. Natural population analysis. *J. Chem. Phys.* **1985**, *83*, 735–746.
55. Reed, A.E.; Curtiss, L.A.; Weinhold, F. Intermolecular interactions from a natural bond orbital, donor-acceptor viewpoint. *Chem. Rev.* **1988**, *88*, 899–926.
56. Frisch, M.J.; Trucks, G.W.; Schlegel, H.B.; Scuseria, G.E.; Robb, M.A.; Cheeseman, J.R.; Scalmani, G.; Barone, V.; Petersson, G.A.; Nakatsuji, H.; et al. *Gaussian 16, Revision A.03*; Gaussian, Inc.: Wallingford, CT, USA, 2016.
57. Dennington, R.; Keith, T.A.; Millam, J.M. *GaussView*, 6th ed.; Semichem Inc.: Shawnee Mission, KS, USA, 2016.
58. Noury, S.; Krokidis, X.; Fuster, F.; Silvi, B. Computational tools for the electron localization function topological analysis. *Comput. Chem.* **1999**, *23*, 597–604.
59. Lu, T.; Chen, F. Multiwfn: A multifunctional wavefunction analyzer. *J. Comp. Chem.* **2012**, *33*, 580-592.
60. AIMAll (Version 19.10.12), Keith, T.A. TK Gristmill Software, Overland Park KS, USA, 2019 (aim.tkgristmill.com)